Supplementary Information (SI) for ChemComm.
This journal is © The Royal Society of Chemistry 2026

Electronic Supplementary Information

Solvation Regulation and Interfacial Adsorption by Ethanolamine-Based Eutectic Electrolyte Toward Byproducts-Free Zinc Anode

Mengya Wang,[a] Haonan Zheng,[a] Hui Zhang,[a] Gaorong Han,[a] Wei-Qiang Han,[a] Hangjun Ying[a*]

a. School of Materials Science and Engineering, Zhejiang University, Hangzhou 310027, China. E-mail: yinghangjun@zju.edu.cn

Experimental materials and methods

Preparation of electrolyte

Zinc trifluoromethanesulfonate ($Zn(OTf)_2$, Macklin, 98%) and ethanolamine (EA, Sigma-Aldrich, ≥99.0%, GC) were used without further purification. 1 M (mol L^{-1}) $Zn(OTf)_2$ was synthesized by dissolving $Zn(OTf)_2$ in deionized water, EA-based hydrated eutectic electrolytes were generated via mixing H_2O and EA at different volume ratios (3:2, 1:1, 1:2, 1:4), and dissolving 1 M $Zn(OTf)_2$ in the mixture. 1 M $Zn(OTf)_2$ in H_2O: EA= 3:2 (volume ratio) was denoted as HE32 electrolyte.

Electrode preparation

The purchased Zn foil (thickness: 100 μm, purity: 99.999%, Tianjin EVS Chemical Technology Co., Ltd.) was polished with a plastic film sandpaper and washed with ethanol to remove the passivation layer. Then, the Zn foil was cut into discs (φ = 14 mm) to be used as a Zn electrode. The Cu foil (thickness: 20 μm, purity: 99.999%, Hefei Wenghe Metal Materials Co., Ltd) was cut into discs (φ = 14 mm) to be used as a Cu electrode. The cathode was prepared by mixing active carbon (AC, BP2000, CABOT), Super-P, and Polytetrafluoroethylene (PTFE) in alcohol with a mass ratio of 85:5:10, stirring the mixture in mortar for 15~30 mins to form uniform lump slurry. Then, rolling the lump slurry on stainless steel (SS) and drying at 60 °C in oven overnight. At last, the cathode was obtained by cutting the foil with 2.7~3 mg cm^{-2} AC into discs (φ = 14 mm).

Characterization of materials

The morphology of Zn anode after saturation and cycles is observed using scanning electron microscopy (SEM, ZEISS Sigma 360), coupled with energy-dispersive X-ray spectroscopy (EDS) to analyze surface elemental distribution. The element of Zn anode was obtained using a powder X-ray

diffraction (XRD, Rigaku Mini Flex 600) with Cu K_α radiation (λ = 1.54065 Å). The differential scanning calorimetry (DSC) analysis was conducted on TA DSC 2500 to measure the glass transition temperature (T_g) and melting point (T_m) of electrolytes at nitrogen (N_2) atmosphere with a heating rate of 10 °C min^{-1} from -120 °C to 25 °C. The intermolecular interaction of electrolytes was detected by Fourier transform infrared spectroscopy (FT-IR, Thermo Scientific Nicolet iS20) with the wavenumber from 4000 to 400 cm^{-1} and the resolution of 0.01 cm^{-1}. Raman spectra were collected on a HORIBA JY LabRAM HR Evolution using an excitation laser beam with a wavelength of 532 nm. The X-ray photoelectron spectroscopy (XPS, Thermo Scientific K-Alpha) was used to analyze the chemical composition on Zn anode surface after cycling.

Electrochemical measurements

Zn||Zn cells, Zn||Cu cells, and Zn||AC cells were assembled in CR2032 coin cells, the assembling pressure was about 750 Psi. All the cells were assembled in the open-air atmosphere using glass fiber (GF/D, Whatman) as the separator, using prepared electrolyte for 60 uL to saturate the electrolyte. Galvanostatic charge-discharge (GCD) were all carried out on a LAND-CT2001A instrument at 25 °C. All electrochemical measurements were depended on the Salartron 1400 electrochemical workstation. If there was no special presentation, the reference electrode below was the Zn^{2+}/Zn electrode. The reversibility of Zn deposition was tested by cyclic voltammetry (CV) of Zn||Cu cells from -0.2 to 0.6 V at 1 mV s^{-1}.

The ionic conductivity (σ) of electrolytes was measured using electrochemical impedance spectroscopy (EIS) method in SS||SS coin cell with the frequence from 10^6 Hz to 0.1 Hz and the AC amplitude of 10 mV. The calculation formula of ionic conductivity was shown in the Equation 1:

$$\sigma = \frac{L}{RS} \tag{1}$$

where L represented the thickness of saturated GF membrane, obtained by dissembling the cells and gauge the thickness, R is the electrolyte resistance obtained from the EIS results and S is the area of SS electrode with a diameter of 15.6 mm.

The average CE with a Zn reservoir on Cu substrate of different electrolytes was measured using Zn||Cu cells. 5 mAh cm^{-2} Zn was first deposited onto and stripped from Cu substrate in the first cycle at the current density of 1 mA cm^{-2} with the charging cutoff voltage of 0.5 V. Then, 5 mAh cm^{-2} Zn was deposited onto Cu substrate as the Zn reservoir (denoted as Q_r). Then, 1 mA cm^{-2}/1 mAh cm^{-2}

(20% capacity of the Zn reservoir, denoted as Q_c) was applied for the stripping-depositing of Zn in the following 30 cycles. At last, the cells were charged to 0.5 V versus Zn^{2+}/Zn to strip Zn in the 31st cycle (denoted as Q_s). The average CE is calculated by the Equation 2.

$$CE = \frac{Q_s + 30Q_c}{Q_r + 30Q_c} \times 100\% \quad (2)$$

The electric double-layer capacitance (C_{dl}) is calculated by analyzing the non-Faraday interval of the double-layer capacitor current in CV curves at different scan rates. A linear fitting method is employed to determine the C_{dl} value.

$$i_c = dq/dt = d(C_{dl}\varphi)/dt = C_{dl}(d\varphi/dt) + \varphi(dC_{dl}/dt)$$

$$dC_{dl}/dt = o,\ d\varphi/dt = v$$

The double-layer current (i_c) is related to C_{dl} and the scan rate (v) by the equation $i_c = C_{dl} * v$. To determine the capacitance, the slope of the linear fitting of i_c versus v is calculated. In this study, $i_c = (i_{0v+} - i_{0v-})/2$, where i_{0v+} and i_{0v-} represent the average values of the positive scan and negative scan at 0 V, respectively. This selection allows for a more accurate description of i_c.

Differential capacitance was collected by processing the EIS results of Zn||Cu cells, where Cu was utilized as the working electrode. The frequency was 6 Hz, the amplitude was 10 mV, AND the scan rate is 1 mV s^{-1}. The differential capacitance curve was calculated from the following equation:

$$C = -\frac{1}{2\pi f Z_{im}} \quad (3)$$

where C is differential capacitance, f is the frequency, and Z_{im} the is the imaginary part of impedance.

CA coupling EIS measurement of Zn||Zn cells was conducted for 10 cycles, each cycle contains a CA, a rest for 2 min, and an EIS test. Under a fixed voltage of -150 mV, the CA test lasts for 5 min. The amplitude of EIS is 10 mV, and the frequency range is from 10^6 to 0.01 Hz.

Density Functional Theory (DFT) calculations

The electrostatic potentials and HOMO/LUMO energy levels of H_2O and EA were calculated in Gaussian 16 software package. Geometric optimization and frequency calculations of components were performed at the B3LYP/6-311+g(d, p) level.

Calculations of adsorption energies were carried out within the DFT framework utilizing the CP2K package. The exchange-correlation interactions were described by the PBE functional, supplemented by the DFT-D3(BJ) correction to account for long-range van der Waals forces. Ionic

cores were treated using GTH-PBE pseudopotentials, while valence electrons were expanded with DZVP-MOLOPT-SR-GTH basis sets. The auxiliary plane-wave basis was truncated at a cutoff of 400 Ry with a relative cutoff of 55 Ry. Surface slab models were established under 2D periodic boundary conditions, separated by a sufficient vacuum layer along the surface normal to prevent spurious interactions. Integration over the Brillouin zone was performed using a 3 × 3 × 1 Monkhorst-Pack grid. Structural relaxations continued until the residual forces on all atoms dropped below 0.02 eV $Å^{-1}$. During this process, the bottom atomic layers of the slab were constrained, whereas the top surface layers and the adsorbed solvent molecules were allowed to fully relax. The adsorption energy was calculated by:

$$E_{ads} = E_{total} - E_{mol} - E_{slab} \quad (3)$$

where E_{total}, E_{mol} and E_{slab} represent the total energies of the optimized solvent-slab system, the isolated solvent molecule, and the clean slab, respectively. All energies were calculated using the same computational settings. The structural models were visualized using the VESTA software.

Molecular dynamic (MD) simulation

MD simulations were carried out using the GROMACS package to explore the interaction of ions and solvent molecules. The specific compositions of ions and solvents are detailed in **Table S1**. The OPLS-AA force field was utilized for $Zn(OTf)_2$ and solvent molecules, whereas the SPC/E model was selected to represent H_2O molecules. Partial charges for the OTf^- anion were calculated using the RESP method and the 1.2*CM5 method was employed to assign charges for neutral solvent molecules. Short-range van der Waals and electrostatic interactions were truncated at 1.0 nm under the Verlet cutoff scheme with the Particle Mesh Ewald (PME) method handling long-range electrostatics. Following energy minimization, the systems underwent a 10 ns equilibration in the NPT ensemble (298.15 K, 1 bar) using the V-rescale thermostat and C-rescale barostat with a 1 fs time step. A subsequent 20 ns production run was executed employing the Nosé-Hoover thermostat and Parrinello-Rahman barostat. Finally, an additional 10 ns simulation in the NVT ensemble was performed to generate trajectories for calculating radial distribution functions (RDFs) and coordination numbers (CNs). All visualization and trajectory analyses were completed using VMD.

Self-Diffusion Coefficient: Firstly, the mean square displacement (MSD) measures were recorded on the following equation:

$$MSD(t) = <|r(t) - r(0)|^2> \quad (4)$$

Then, the self-diffusion coefficient of Zn^{2+} (D_{Zn2+}) was calculated by using the following equation:

$$D = \frac{1}{6}\lim_{t\to\infty}\frac{MSD(t)}{t} \quad (5)$$

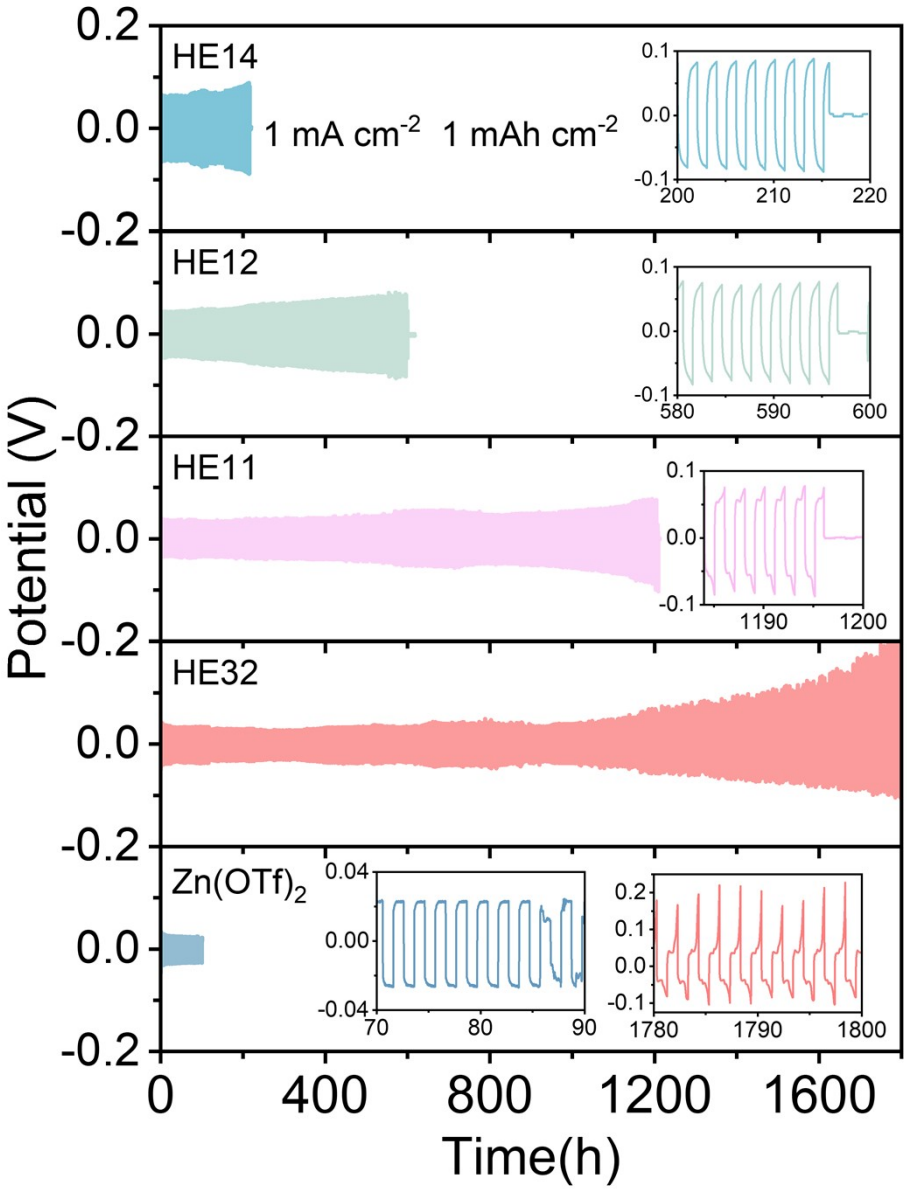

Figure S1 Cyclic performance of Zn||Zn cells at 1 mA cm^{-2}/1 mAh cm^{-2} with different electrolytes.

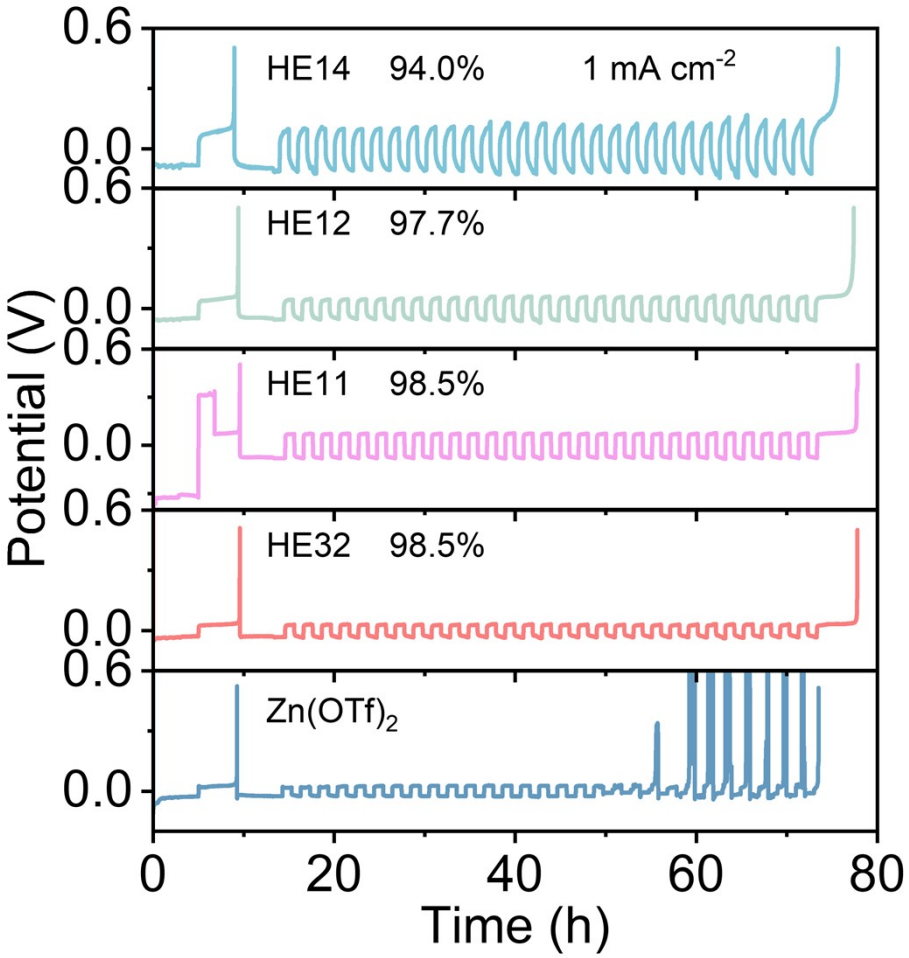

Figure S2 Average CEs of Zn||Cu cells using "reservoir half-cell" galvanostatic protocol.

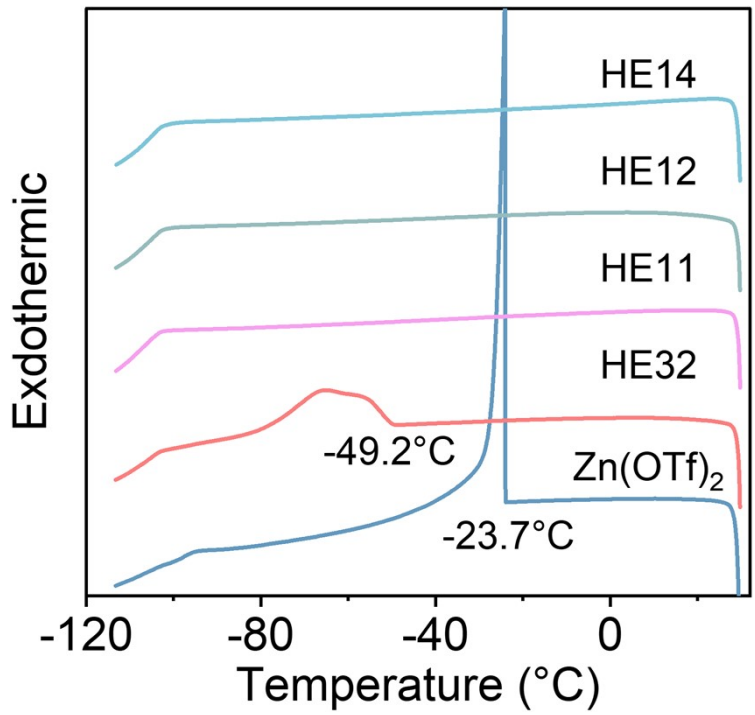

Figure S3 DSC curves from -120 °C to 30 °C with a heating rate of 10 °C min^{-1}.

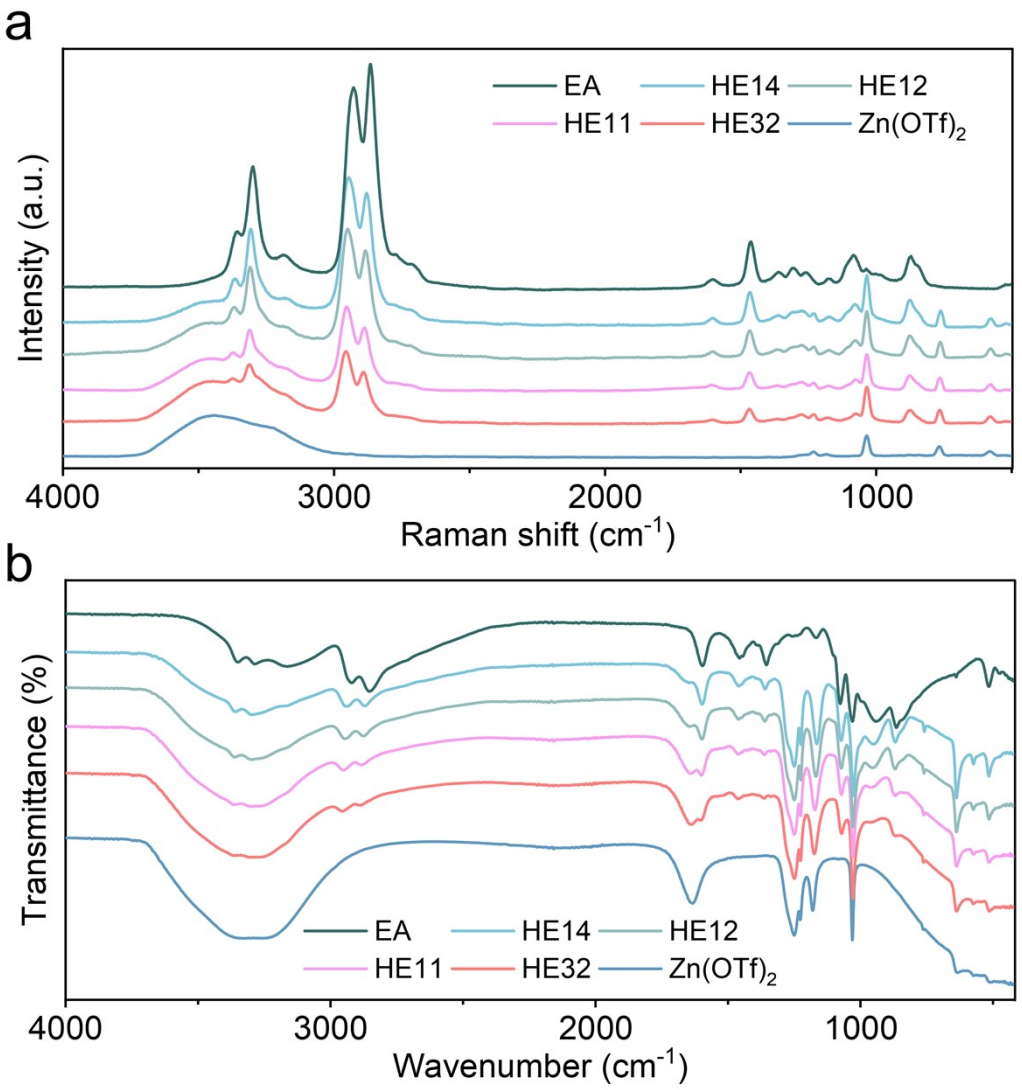

Figure S4 (a) Raman and (b) FT-IR spectra of different electrolytes.

Table S1 The initial configuration setup of MD simulation.

System	Number of $Zn(OTf)_2$	Number of H_2O	Number of EA
$Zn(OTf)_2$ electrolyte	100	5556	
HE32 electrolyte	100	3333	665

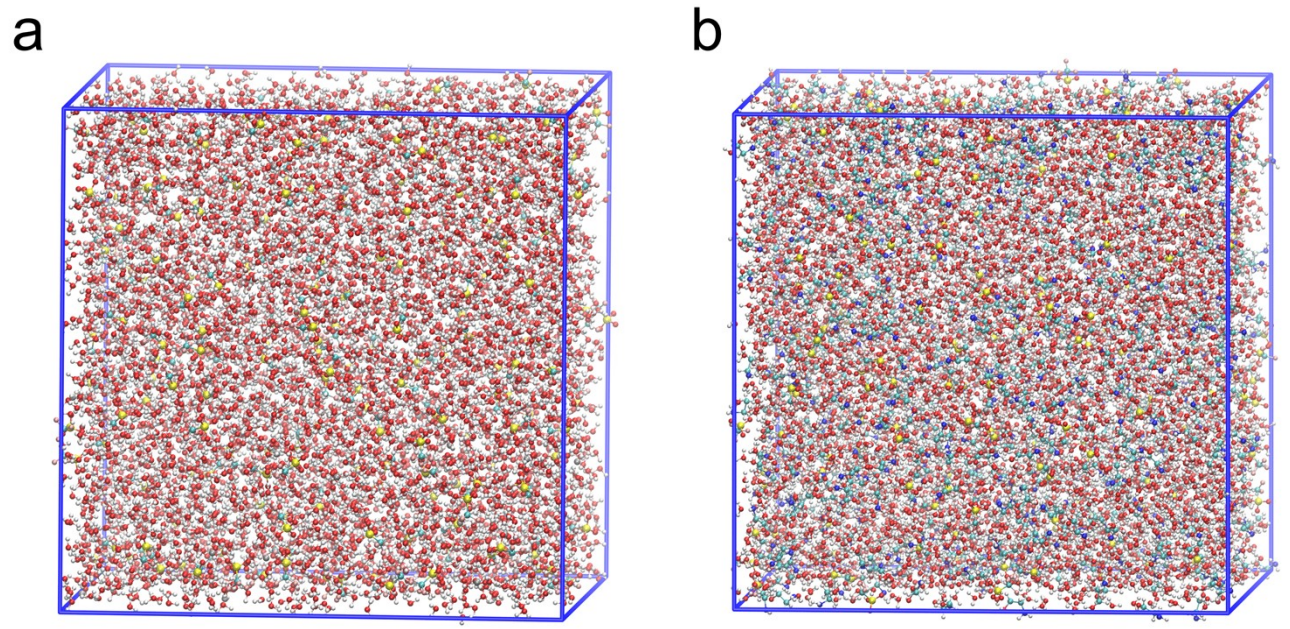

Figure S5 Snapshots of MD simulation in (a) $Zn(OTf)_2$ and (b) HE32 electrolytes.

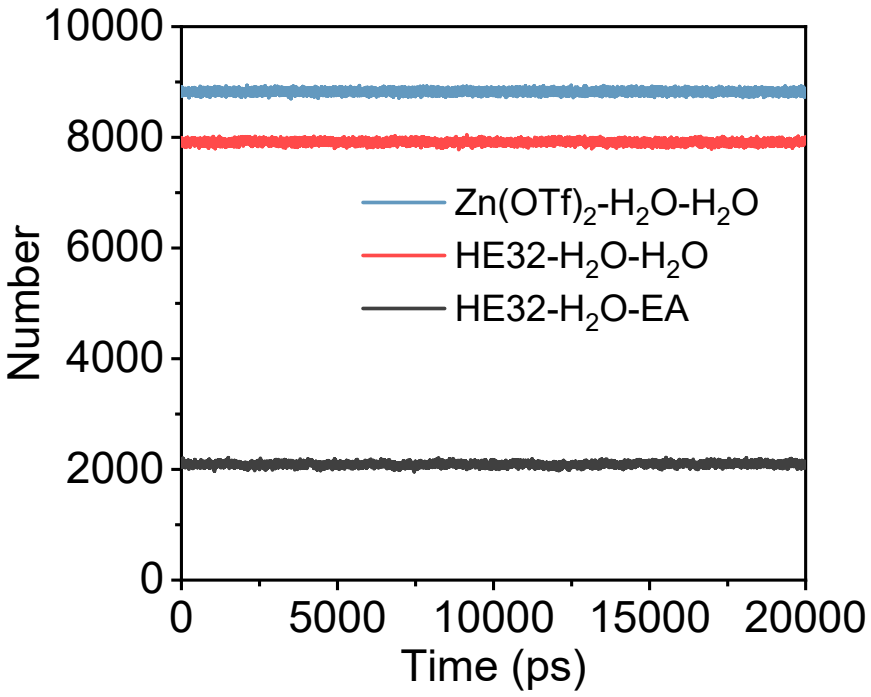

Figure S6 Hydrogen bond number H_2O-H_2O and H_2O-EA interaction in $Zn(OTf)_2$ and HE32 electrolyte.

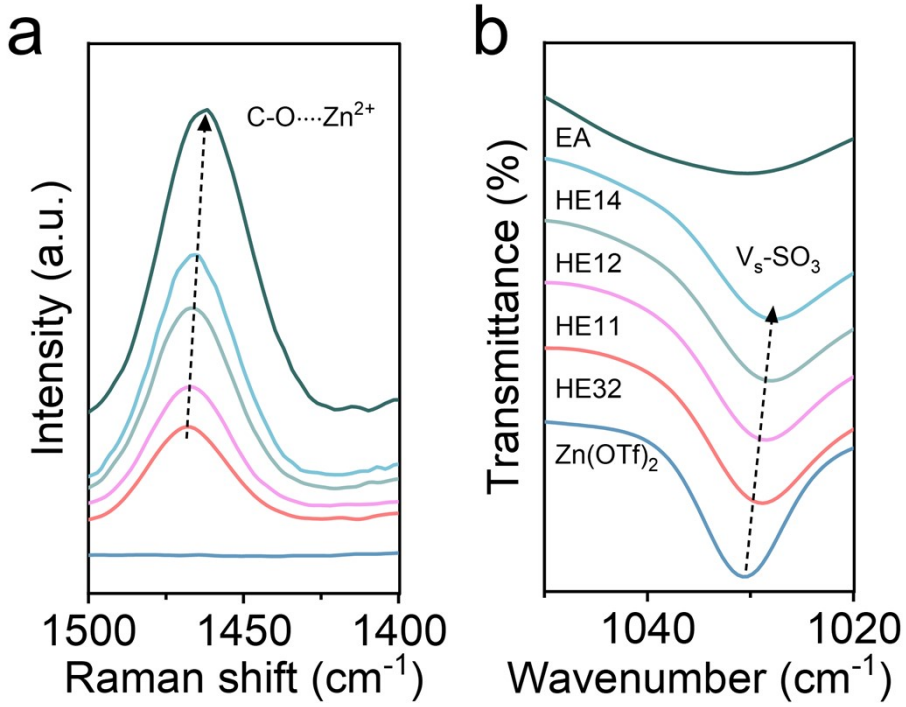

Figure S7 (a) Raman spectra at 1500~1400 cm^{-1}, and (b) FT-IR spectra at 1050~1020 cm^{-1}.

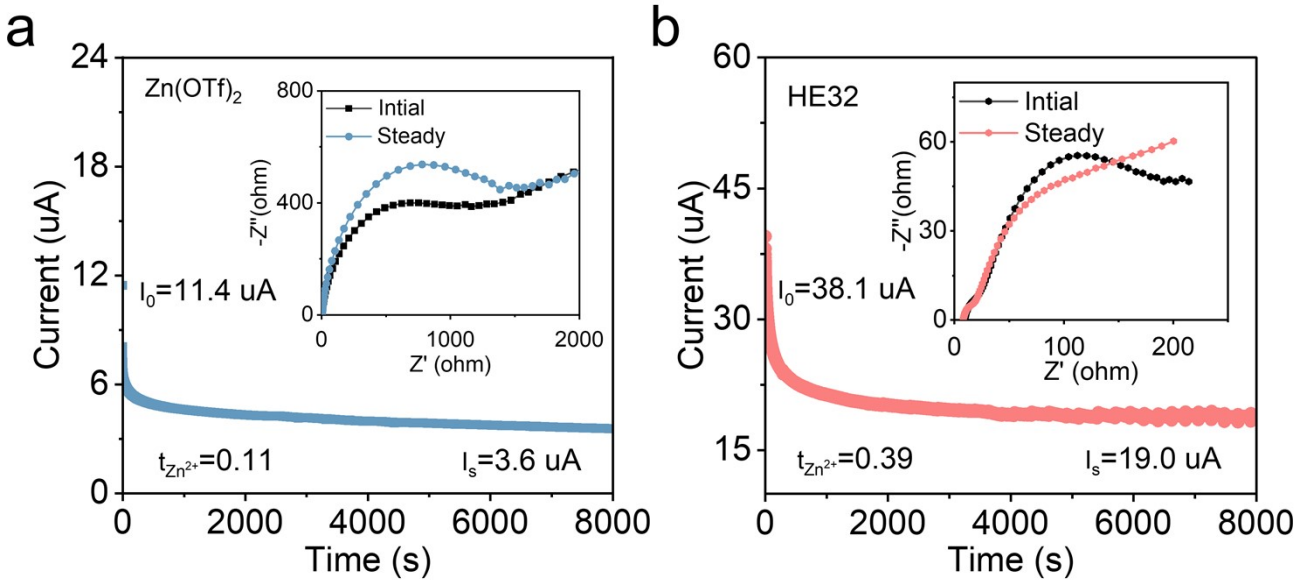

Figure S8 Zn^{2+} transference number in (a) $Zn(OTf)_2$ and (b) HE32 electrolytes.

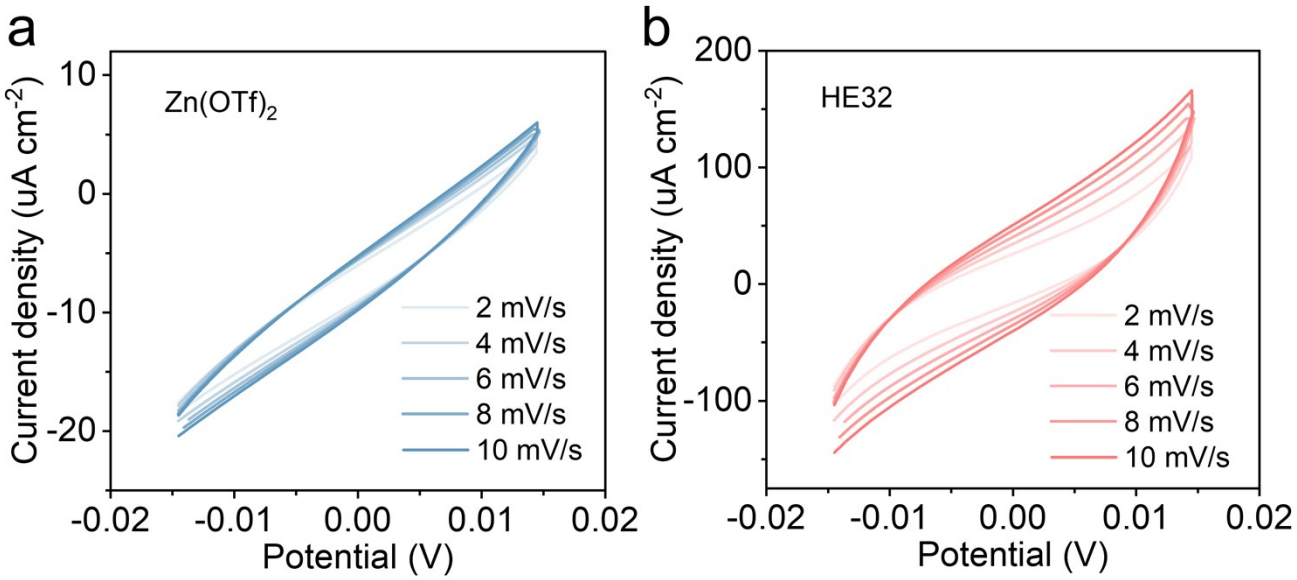

Figure S9 CV curves of Zn||Zn cells with (a) $Zn(OTf)_2$ and (b) HE32 electrolytes from -15 mV to 15 mV at varied scan rates.

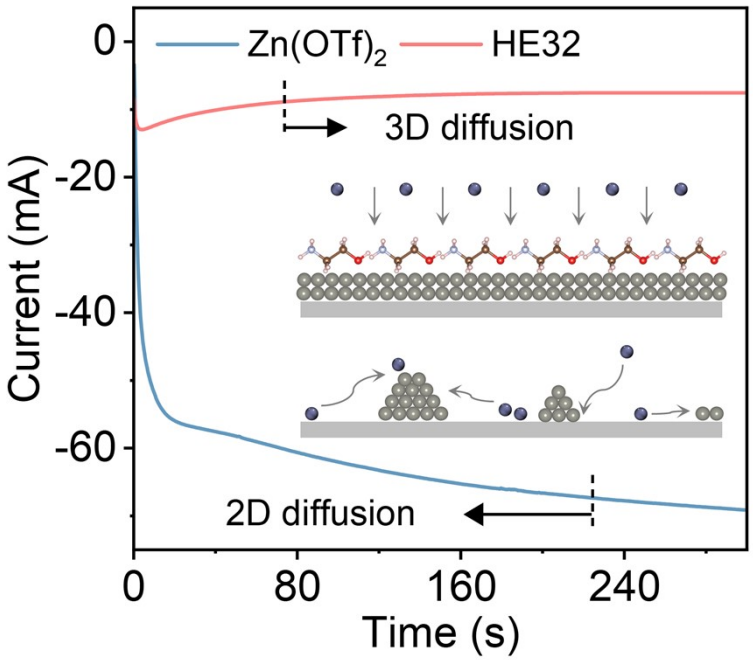

Figure S10 CA curves of Zn||Zn cells under a fixed potential of -150 mV.

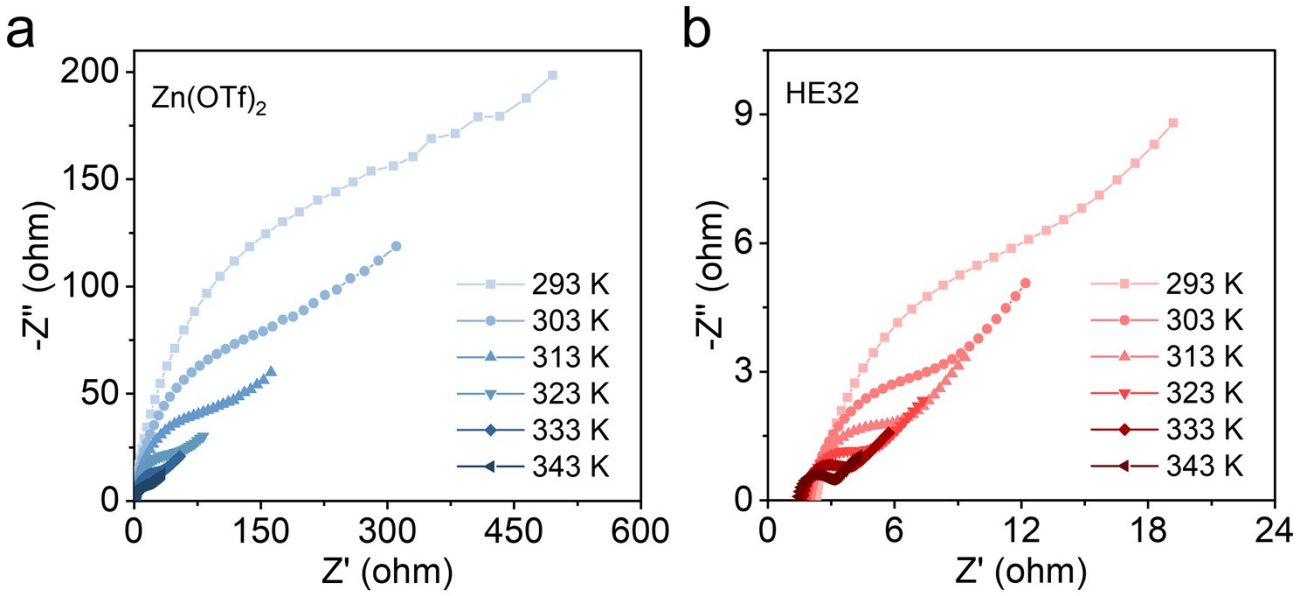

Figure S11 Nyquist plots of Zn||Zn cells with (a) $Zn(OTf)_2$ and (b) HE32 electrolytes at 293 K~ 343 K.

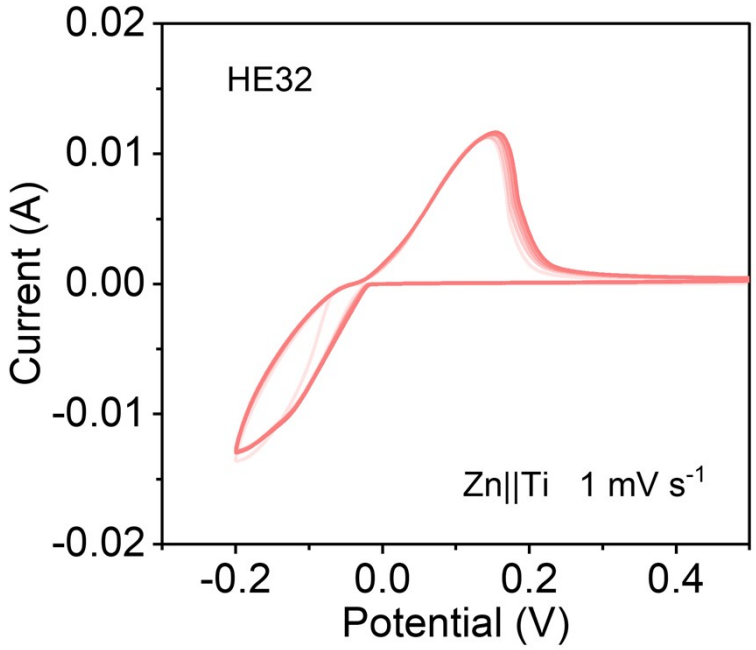

Figure S12 CV curves of Zn||Ti cells with HE32 electrolyte at 1 mV s^{-1} for 5 cycles.

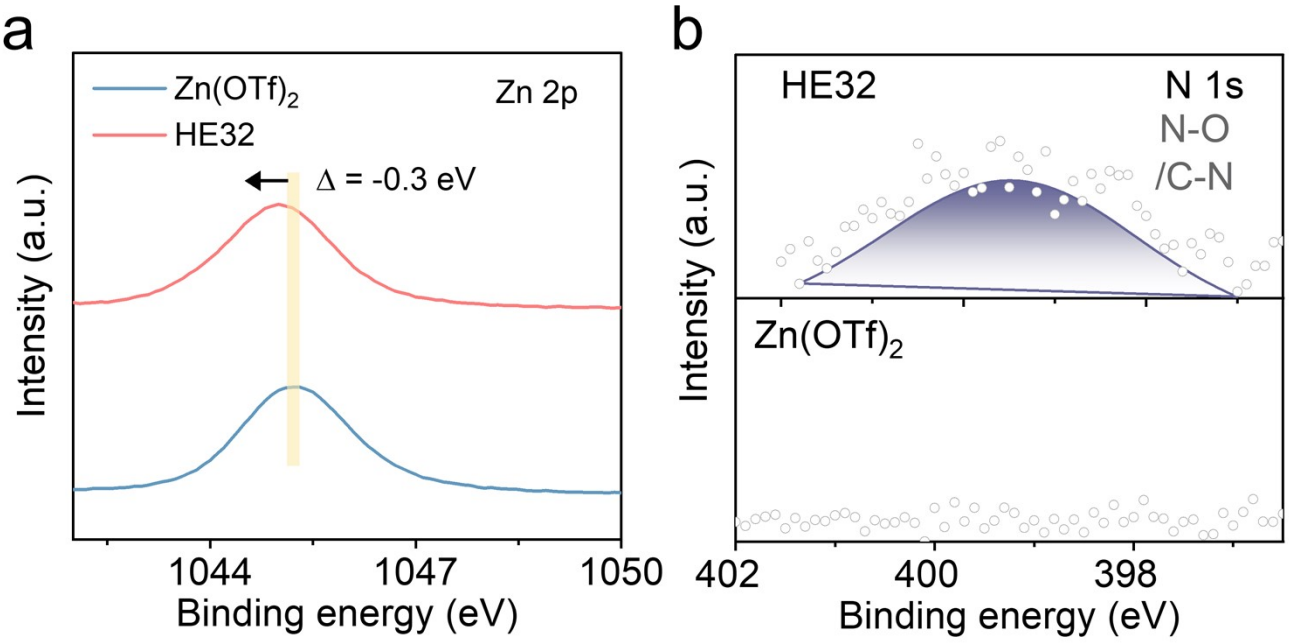

Figure S13 (a) Zn 2p, (b) N 1s fine peaks of cycled Zn anode at 1 mA cm^{-2}/1 mAh cm^{-2} for 100 h.

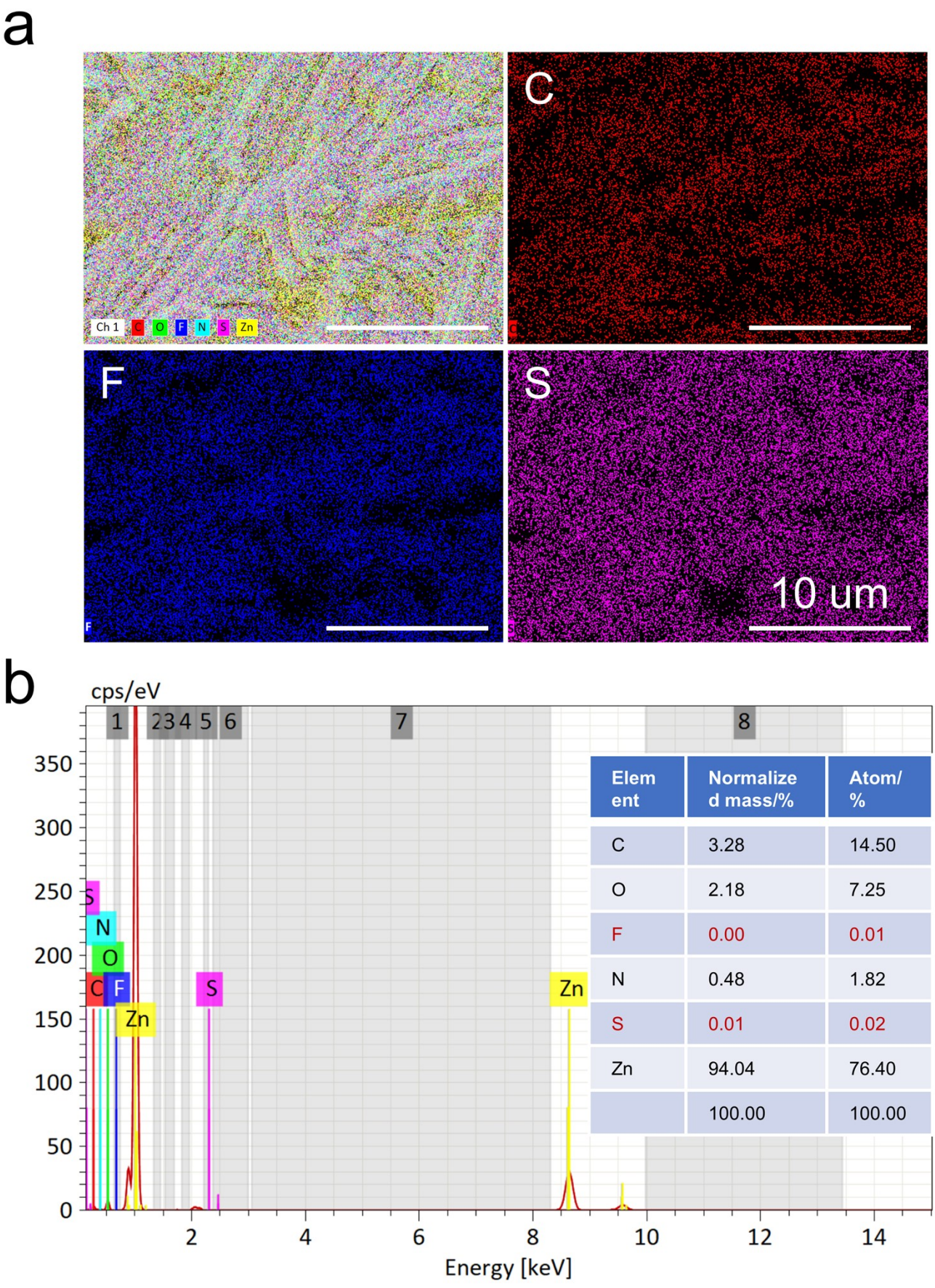

Element	Normalized mass/%	Atom/ %
C	3.28	14.50
O	2.18	7.25
F	0.00	0.01
N	0.48	1.82
S	0.01	0.02
Zn	94.04	76.40
	100.00	100.00

Figure S14 (a) Mapping results of C, F, and S elements of cycled Zn anode in HE32 electrolyte, and

corresponding (b) energy spectra with specific element proportion.

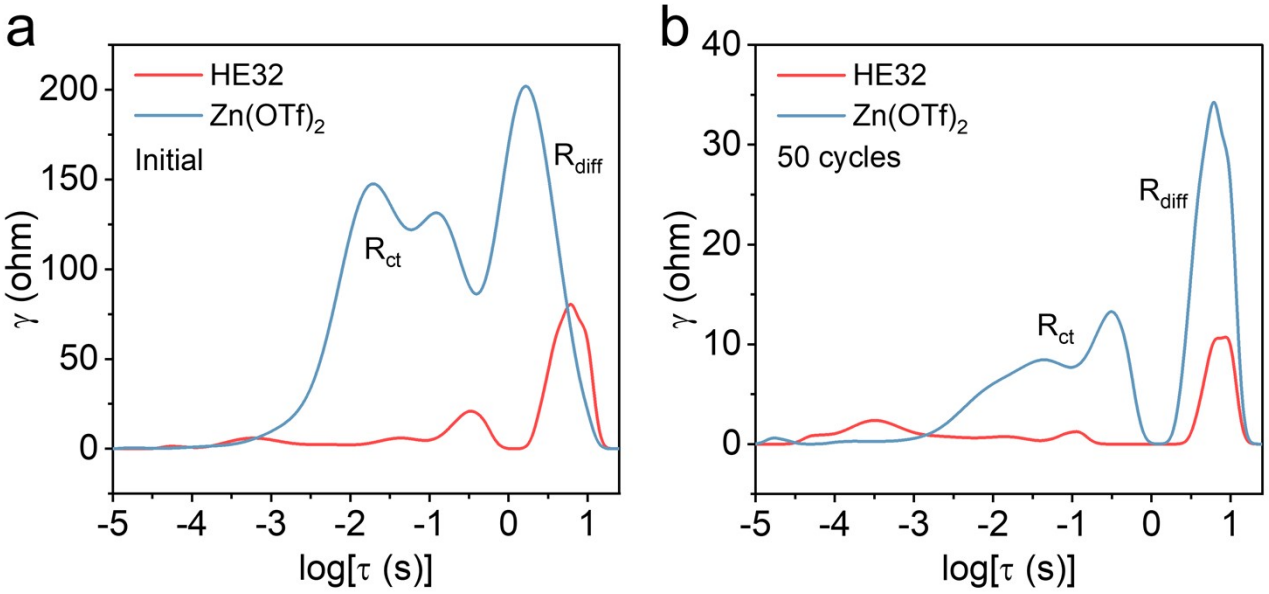

Figure S15 DRT plots of Zn||Zn cells with $Zn(OTf)_2$ and HE32 electrolytes at initial stage and after 50 cycles.

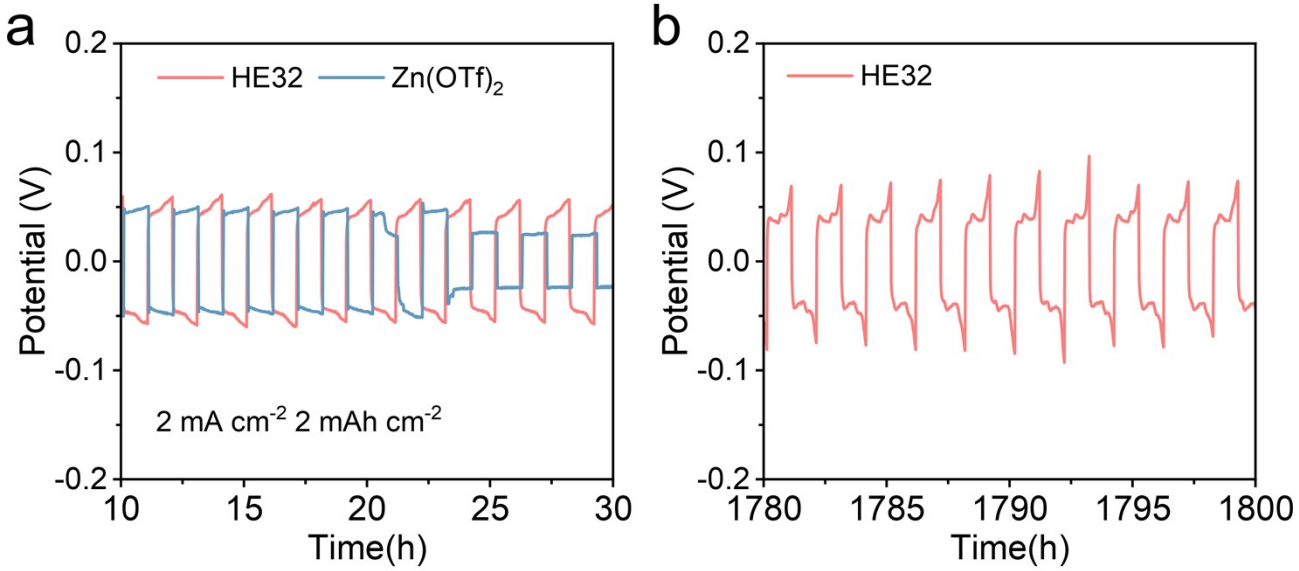

Figure S16 Voltage profiles of Zn||Zn cells at (a) 10~30 h and (b) 1780~1800 h.

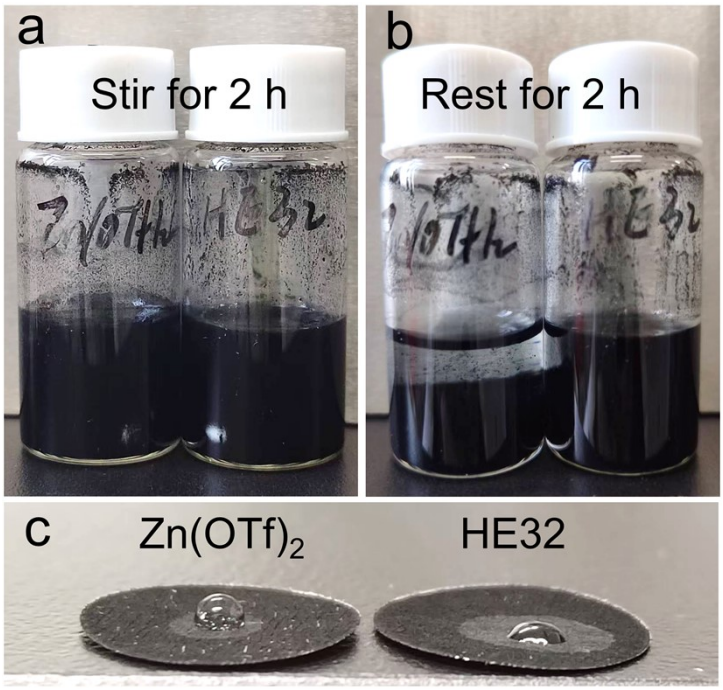

Figure S17 Optical images of 10 mg AC powder in 3 mL $Zn(OTf)_2$ and HE32 electrolytes (a) after stirring for 2 h and (b) then resting for 2 h. (c) Optical images of $Zn(OTf)_2$ (left) and HE32 (right) electrolytes on AC cathode.

AC powder disperses uniformly in $Zn(OTf)_2$ and HE32 electrolytes after mechanical stirring. While after resting for 2 h, $Zn(OTf)_2$ electrolyte cannot maintain steady dispersion liquid, the AC cathode subsides gradually, verifying the unfavored wettability. In reverse, AC cathode in HE32 electrolyte attains uniform dispersion liquid. Meanwhile, a faster saturation speed and an apparent lower contact angle of HE32 electrolyte on AC electrode are observed, validating the better wettability of HE32 electrolyte.

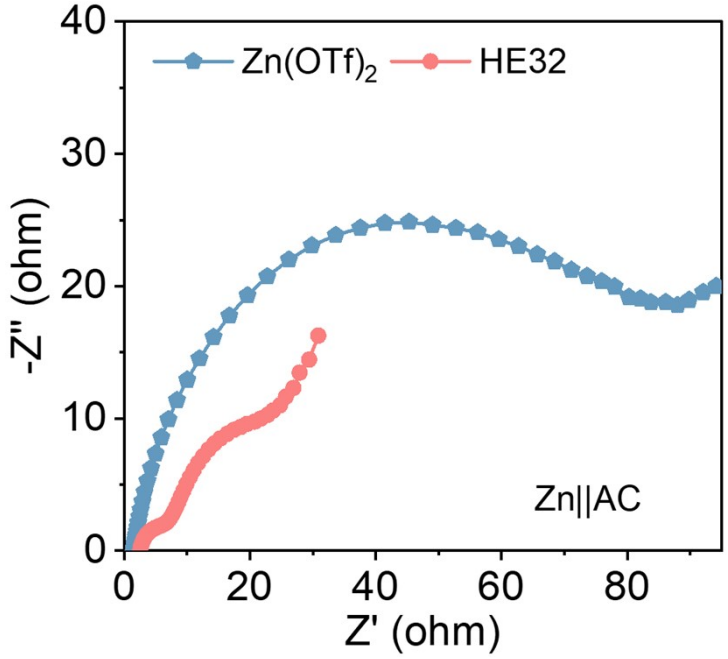

Figure S18 Nyquist plots of Zn||AC full cells with $Zn(OTf)_2$ and HE32 electrolytes.

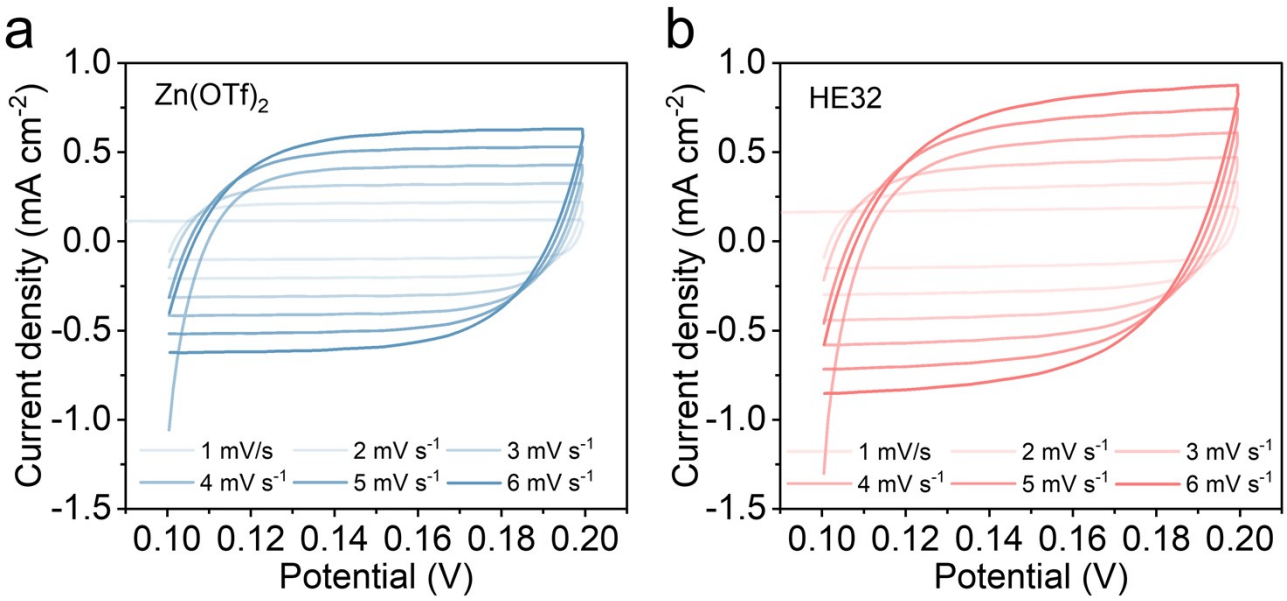

Figure S19 CV curves of AC||AC symmetric cells at different scan rates with (a) $Zn(OTf)_2$ and (b) HE32 electrolytes at 0.1~0.2 V.

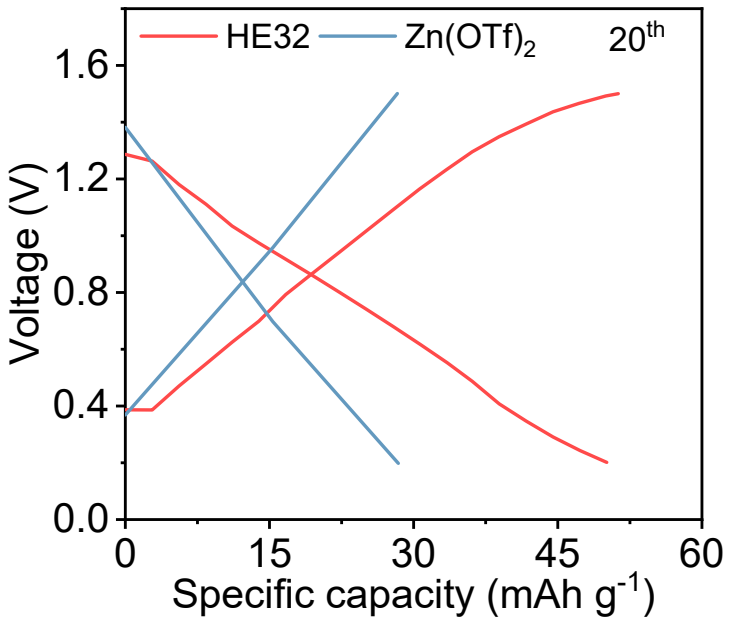

Figure S20 The voltage profiles of Zn||AC batteries at 1 A g^{-1} for the 20th cycle.

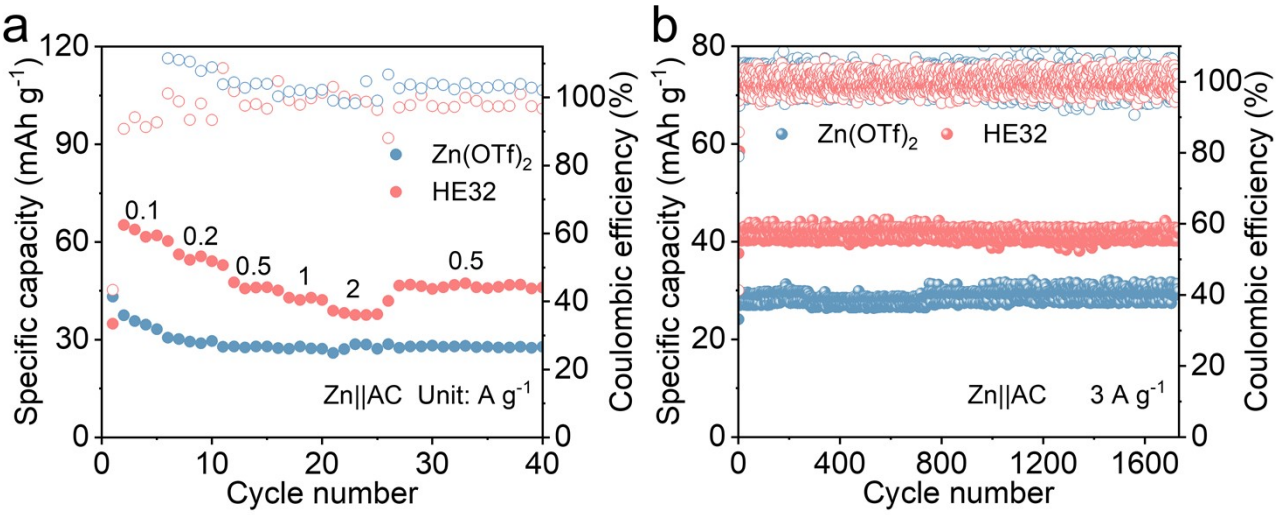

Figure S21 (a) Rate performance and cycling performance at 3 A g^{-1} of different electrolytes.

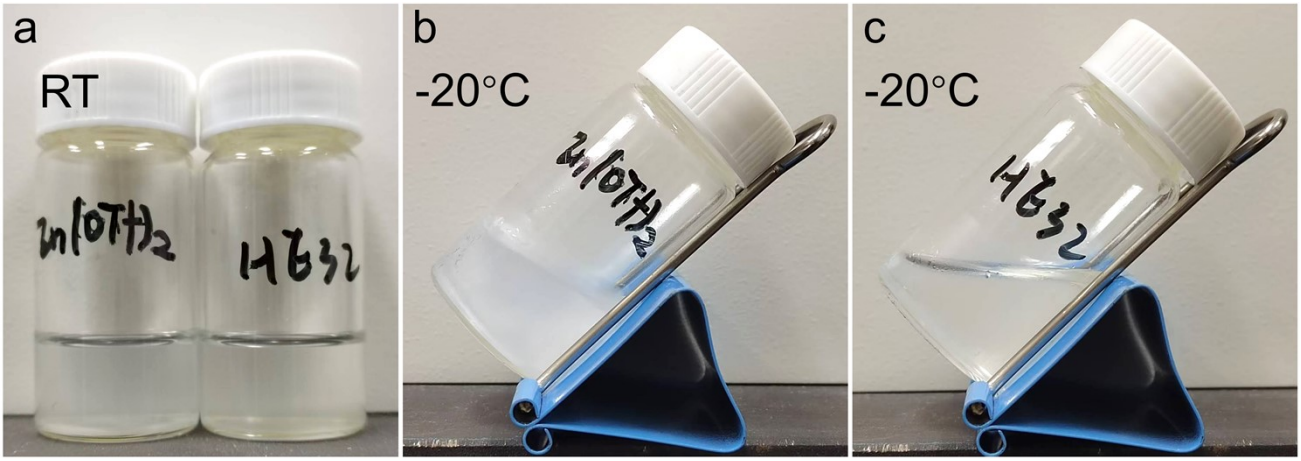

Figure S22 (a) Optical images of $Zn(OTf)_2$ and HE32 electrolytes at room temperature (RT). The (b) freezing state of $Zn(OTf)_2$ and the (c) fluid state of HE32 electrolyte at -20 °C.

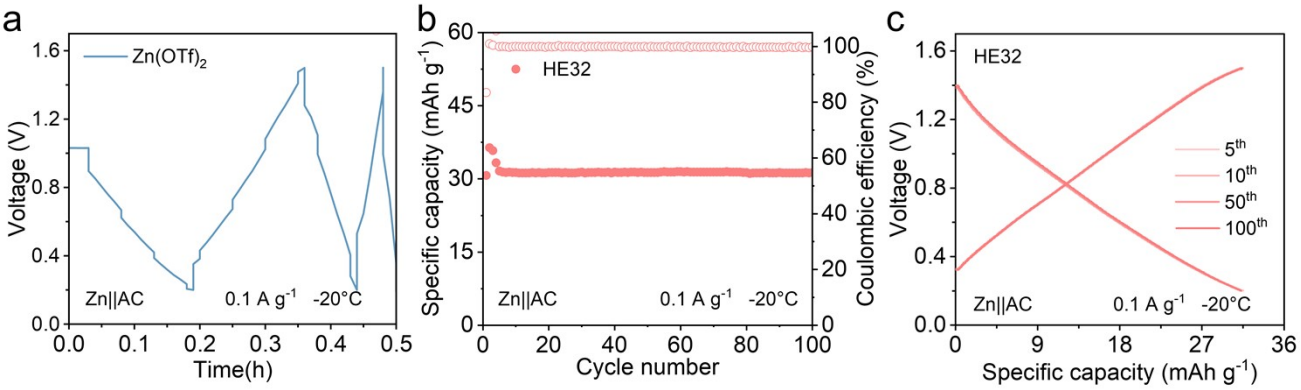

Figure S23 (a) Voltage-time profile of Zn||AC full battery with $Zn(OTf)_2$ electrolyte at -20°C, (b) cycling performance of Zn||AC full battery with HE32 electrolyte at -20 °C, 0.1 A g^{-1} and (c) corresponding voltage-capacity profiles.